

Wavelets on the interval with optimal localization

Original

Wavelets on the interval with optimal localization / GRIVET TALOCIA, Stefano; Tabacco, Anita Maria. - In: MATHEMATICAL MODELS AND METHODS IN APPLIED SCIENCES. - ISSN 0218-2025. - STAMPA. - 10:3(2000), pp. 441-462. [10.1142/S0218202500000252]

Availability:

This version is available at: 11583/1406319 since:

Publisher:

World Scientific

Published

DOI:10.1142/S0218202500000252

Terms of use:

This article is made available under terms and conditions as specified in the corresponding bibliographic description in the repository

Publisher copyright

(Article begins on next page)

WAVELETS ON THE INTERVAL WITH OPTIMAL LOCALIZATION

STEFANO GRIVET-TALOCIA

*Dipartimento di Elettronica, Politecnico di Torino
Corso Duca degli Abruzzi, 24 - 10129 Torino - Italy*

ANITA TABACCO

*Dipartimento di Matematica, Politecnico di Torino
Corso Duca degli Abruzzi, 24 - 10129 Torino - Italy*

(Leave 1 inch blank space for publisher.)

This paper introduces a novel construction of wavelets on the unit interval. With this construction explicit upper bounds for the length of the modified border wavelets filters can be given. This insures a good localization of the border wavelets when a triangular biorthogonalization scheme is employed. The resulting wavelet bases are then well suited for the adaptive solution of partial differential equations.

1. Introduction

Wavelets provide very efficient multilevel decompositions of signals, functions, and operators. Properly designed algorithms may lead to solution schemes for PDE's characterized by a reduced computational complexity with respect to more standard discretizations at no loss of accuracy. Among the various applications in this field we recall multilevel preconditioning, compression of discretization matrices and adaptivity (see Refs. 11, 6, 9, and references therein).

One of the key properties of wavelets is translation invariance. This leads to the construction of multilevel decompositions naturally defined on the full real line, or on bounded domains with periodic boundary conditions. However, most of the applications require the solution of PDE's within a bounded domain with possibly complex boundary conditions. Therefore, if wavelets are to be used, special care must be taken in the construction of wavelet bases inherently defined on bounded domains. The simplest case is represented by wavelet bases on the unit interval $(0, 1)$. These can also be used as a building block to construct wavelet bases on multidimensional domains of complex shape.^{4,5,14}

We concentrate our attention to the construction of biorthogonal wavelet bases on the half-line $(0, +\infty)$ and, subsequently on the unit interval. The construction of such bases originates naturally by wavelets defined on the whole line by introducing suitable modifications to account for the edges of the domain. We focus on

biorthogonal systems rather than on orthogonal ones, like the famous Daubechies' compactly supported orthogonal wavelets,¹⁵ because the former can be chosen to have useful properties, like, e.g., compact support and central symmetry. As an example we can cite the biorthogonal B-splines wavelets.⁷ All orthogonal systems are a particular case of the more general biorthogonal setting.

Many constructions of orthogonal and/or biorthogonal wavelets on the unit interval or half-line can be found in the literature.^{1,8,12,19} Generally, these constructions do not uniquely determine one particular biorthogonal system, but leave the freedom to insure additional properties of the wavelet bases. In this paper we will exploit this possibility and we will propose a different definition of the border wavelets which seems to be better adapted to the applications.^{17,18} The key advantages of this new construction are a good localization of the modified border wavelets and a short length of the corresponding filters. These two features are of great importance in the construction of adaptive schemes for the solution of PDE's.

The outline of the paper is as follows. In Section 2, we review the main properties of systems on the real line. Moreover, we recall how to construct scaling function spaces on the half-line $(0, +\infty)$ and we describe the structure of their filter matrices. Section 3 is devoted to the construction of biorthogonal systems of wavelets on the half-line, exploiting again their filter matrices. In Section 4, we describe the construction of scaling function and wavelet bases on the unit interval starting from the construction on the half-line. We show, in Section 5, how we perform the biorthogonalization process on both the border scaling functions and wavelets in order to preserve a short filter length and a good localization. Finally, we report in Section 6 an application illustrating the optimal localization provided by the proposed construction.

2. Preliminary

In this section we review those aspects of the construction of scaling functions and wavelets that will be extensively used in the following. In Section 2.1 we recall the main properties for biorthogonal systems of compactly supported wavelets generating multilevel decompositions of $L^2(\mathbb{R})$ (see, e.g., Refs. 7, 3, 2). This setting will be a necessary framework for the construction of biorthogonal wavelet systems on the half line and on the unit interval. In Section 2.2 we describe how to construct scaling function spaces for the half-line $\mathbb{R}^+ = (0, +\infty)$; we follow Refs. 19, 3, where the formal proofs can be found (see also Refs. 1, 12). Finally, in Section 2.3, we draw some considerations on the modified border scaling functions filters, which will be important for the subsequent construction of the border wavelets.

2.1. Biorthogonal decomposition in \mathbb{R}

Scaling functions. Let us consider two compactly supported scaling functions $\varphi, \tilde{\varphi} \in$

$L^2(\mathbb{R})$ satisfying the following refinement equations with finite real filters h and \tilde{h} ,

$$\varphi(x) = \sqrt{2} \sum_{n=n_0}^{n_1} h_n \varphi(2x-n), \quad \tilde{\varphi}(x) = \sqrt{2} \sum_{n=\tilde{n}_0}^{\tilde{n}_1} \tilde{h}_n \tilde{\varphi}(2x-n). \quad (2.1)$$

Without loss of generality we will assume $\tilde{n}_0 \leq n_0 \leq 0 \leq n_1 \leq \tilde{n}_1$ so that $\text{supp } \varphi = [n_0, n_1] \subseteq \text{supp } \tilde{\varphi} = [\tilde{n}_0, \tilde{n}_1]$. If this is not the case, the role of the primal and the dual functions can be exchanged. From now on, we will only give details for the primal setting. The dual construction, herewith indicated with a tilde $\tilde{\cdot}$, follows by analogy.

Setting for $j, k \in \mathbb{Z}$, $\varphi_{jk}(x) = 2^{j/2} \varphi(2^j x - k)$, we suppose that the biorthogonality relations

$$\langle \varphi_{jk}, \tilde{\varphi}_{j'k'} \rangle_{\mathbb{R}} := \int_{\mathbb{R}} \varphi_{jk}(x) \tilde{\varphi}_{j'k'}(x) dx = \delta_{kk'}, \quad \forall j, k, k' \in \mathbb{Z} \quad (2.2)$$

hold. Moreover, for any $j \in \mathbb{Z}$, the set $\{\varphi_{jk} : k \in \mathbb{Z}\}$ will be a uniformly 2-stable basis for the space

$$V_j = V_j(\mathbb{R}) = \text{span}_{L^2} \{\varphi_{jk} : k \in \mathbb{Z}\} = \left\{ v = \sum_{k \in \mathbb{Z}} \alpha_k \varphi_{jk} : \{\alpha_k\}_{k \in \mathbb{Z}} \in \ell^2 \right\},$$

i.e., there exist two constants $A, B > 0$ such that, for any $v = \sum_k \alpha_k \varphi_{jk} \in V_j$,

$$A \|\{\alpha_k\}_{k \in \mathbb{Z}}\|_{\ell^2} \leq \|v\|_{L^2(\mathbb{R})} \leq B \|\{\alpha_k\}_{k \in \mathbb{Z}}\|_{\ell^2}.$$

This stability relation will be abbreviated in the sequel by $\|v\|_{L^2(\mathbb{R})} \asymp \|\{\alpha_k\}_{k \in \mathbb{Z}}\|_{\ell^2}$. Moreover, due to the biorthogonality relations (2.2), we can write

$$v = \sum_{k \in \mathbb{Z}} \check{v}_{jk} \varphi_{jk} \quad \text{with} \quad \check{v}_{jk} = \langle v, \tilde{\varphi}_{jk} \rangle_{\mathbb{R}}.$$

In addition, $V_j \subset V_{j+1}$, $\bigcap_{j \in \mathbb{Z}} V_j = \{0\}$, $\overline{\bigcup_{j \in \mathbb{Z}} V_j} = L^2(\mathbb{R})$.

Finally, we suppose that there exists an integer $L \geq 1$ so that, locally, the polynomials of degree up to $L-1$ (we will indicate this set \mathcal{P}_{L-1}) are contained in V_j . It is not difficult to show³ that L must satisfy the relation $L \leq n_1 - n_0 - 1$. Similarly, there exists an integer \tilde{L} with analogous properties for the dual system, and satisfying $\tilde{L} \geq L$.

Wavelets. The primal wavelet is defined as

$$\psi(x) = \sqrt{2} \sum_{n=1-\tilde{n}_1}^{1-\tilde{n}_0} g_n \varphi(2x-n), \quad \text{with} \quad g_n = (-1)^n \tilde{h}_{1-n}.$$

Setting $\psi_{jk}(x) = 2^{j/2} \psi(2^j x - k)$, $\forall j, k \in \mathbb{Z}$, and defining similarly the dual wavelets $\tilde{\psi}_{jk}$, then $\langle \psi_{jk}, \tilde{\psi}_{j'k'} \rangle_{\mathbb{R}} = \delta_{jj'} \delta_{kk'}$, $\forall j, j', k, k' \in \mathbb{Z}$. The spaces

$$W_j = \left\{ \sum_{k \in \mathbb{Z}} \alpha_k \psi_{jk} : \{\alpha_k\}_{k \in \mathbb{Z}} \in \ell^2 \right\}, \quad \forall j \in \mathbb{Z},$$

are such that

$$V_{j+1} = V_j \oplus W_j, \quad W_j \perp \tilde{V}_j, \quad \tilde{V}_{j+1} = \tilde{V}_j \oplus \tilde{W}_j, \quad \tilde{W}_j \perp V_j,$$

and satisfy $L^2(\mathbb{R}) = \oplus_{j \in \mathbb{Z}} W_j$. For any $v \in L^2(\mathbb{R})$, this implies the expansion

$$v = \sum_{j,k \in \mathbb{Z}} \hat{v}_{jk} \psi_{jk}, \quad \text{with } \hat{v}_{jk} = \langle v, \tilde{\psi}_{jk} \rangle_{\mathbb{R}}.$$

In addition $\|v\|_{L^2(\mathbb{R})} \asymp (\sum_{j,k \in \mathbb{Z}} |\hat{v}_{jk}|^2)^{1/2}$, $\forall v \in L^2(\mathbb{R})$.

Refinement and reconstruction equations. We recall now some relations that will be useful in the following. The primal scaling functions and wavelets are related by the refinement equations

$$\varphi_{jm} = \sum_{k \in \mathbb{Z}} h_{k-2m} \varphi_{j+1,k}, \quad \forall m \in \mathbb{Z}, \quad (2.3)$$

$$\psi_{jm} = \sum_{k \in \mathbb{Z}} g_{k-2m} \varphi_{j+1,k}, \quad \forall m \in \mathbb{Z}, \quad (2.4)$$

and by the reconstruction equation

$$\varphi_{j+1,k} = \sum_{m \in \mathbb{Z}} \tilde{h}_{k-2m} \varphi_{jm} + \sum_{m \in \mathbb{Z}} \tilde{g}_{k-2m} \psi_{jm}, \quad \forall k \in \mathbb{Z}, \quad (2.5)$$

where $\{\tilde{h}_k\}$ and $\{\tilde{g}_k\}$ are the dual filters. The latter can also be restated as

$$\sum_m [h_{k-2m} \tilde{h}_{n-2m} + g_{k-2m} \tilde{g}_{n-2m}] = \delta_{kn}, \quad \forall k, n \in \mathbb{Z}. \quad (2.6)$$

2.2. *Scaling function spaces for the half-line*

We recall in this section the main steps in the construction of scaling functions on the half-line $(0, +\infty)$. This is derived from an underlying construction on the real line through suitable modifications of the functions that interact with the border $x = 0$. To avoid ambiguity, from now on we will append a suffix $^{\mathbb{R}}$ to all the functions defined on the real line. It will be assumed that all the functions without this suffix are defined on the half-line. Also, for simplicity, we will work on the scale $j = 0$.

Interaction with the border. As we have already mentioned, the guideline underlying the construction is to preserve as much as possible the structure of the decomposition on the real line, and to introduce modifications only for those functions interacting with the boundary $x = 0$. To this end, note that if $k \geq -n_0$, $\varphi_{0k}^{\mathbb{R}}$ has support contained in $[0, +\infty)$. More precisely $\text{supp } \varphi_{0k}^{\mathbb{R}} = [n_0 + k, n_1 + k]$. Let us

fix a nonnegative integer δ and set $k_0^* = -n_0 + \delta$; observe that $k_0^* = \min\{k \in \mathbb{Z} : \text{supp } \varphi_{0k}^{\mathbb{R}} \subseteq [\delta, +\infty)\}$. Let us define

$$V^{(+)} = \text{span } \{\varphi_{0k}^{\mathbb{R}}|_{[0,+\infty)} : k \geq k_0^*\}; \quad (2.7)$$

this space will be identified in a natural way with a subspace of $V_0(\mathbb{R})$ and will not be modified by the subsequent construction.

Polynomial reproduction. To obtain a scaling function space $V_0(\mathbb{R}^+)$ for the half-line, we will add to the basis $\{\varphi_{0k}^{\mathbb{R}}|_{[0,+\infty)} : k \geq k_0^*\}$ of $V^{(+)}$ a finite number of new functions. These functions will be constructed so that the property of reproduction of polynomials is maintained. In fact we know that for any polynomial $p \in \mathcal{P}_{L-1}$ and every fixed $x \in \mathbb{R}$, there is a suitable set of coefficients \check{p}_{0k} such that $p(x) = \sum_{k \in \mathbb{Z}} \check{p}_{0k} \varphi_{0k}^{\mathbb{R}}(x)$. So, if $\{p_\alpha : \alpha = 0, \dots, L-1\}$ is a basis for \mathcal{P}_{L-1} , for every $x \geq 0$, we have

$$p_\alpha(x) = \sum_{k \geq -n_1+1} c_{\alpha k} \varphi_{0k}^{\mathbb{R}}(x) = \sum_{k=-n_1+1}^{k_0^*-1} c_{\alpha k} \varphi_{0k}^{\mathbb{R}}(x) + \sum_{k \geq k_0^*} c_{\alpha k} \varphi_{0k}^{\mathbb{R}}(x), \quad (2.8)$$

where $c_{\alpha k} := \int_{\mathbb{R}} p_\alpha(y) \tilde{\varphi}^{\mathbb{R}}(y-k) dy$, $\alpha = 0, \dots, L-1$. Since the second sum in (2.8) is a linear combination of elements of $V^{(+)}$, in order to locally generate all polynomials of degree $\leq L-1$ on the half-line, we will add to this space all the functions

$$\phi_{0\alpha}(x) = \sum_{k=-n_1+1}^{k_0^*-1} c_{\alpha k} \varphi_{0k}^{\mathbb{R}}|_{[0,+\infty)}(x), \quad \alpha = 0, \dots, L-1. \quad (2.9)$$

It is clear that different bases of \mathcal{P}_{L-1} lead to different functions $\phi_{0\alpha}$. Some remarks on possible choices can be found later in this subsection and in Section 5.

It is not difficult to show that the functions $\{\phi_{0\alpha} : \alpha = 0, \dots, L-1\} \cup \{\varphi_{0k}^{\mathbb{R}}|_{[0,+\infty)}, k \geq k_0^*\}$ are linearly independent. Therefore, it is natural to define

$$V_0(\mathbb{R}^+) = \text{span } \{\phi_{0\alpha} : \alpha = 0, \dots, L-1\} \oplus V^{(+)}.$$

If we rename the internal functions as

$$\phi_{0k} = \varphi_{0, k_0^*+k-L}^{\mathbb{R}}|_{[0,+\infty)} \quad \text{if } k \geq L,$$

we can write in a more compact form

$$V^{(+)} = \text{span } \{\phi_{0k} : k \geq L\} \quad \text{and} \quad V_0(\mathbb{R}^+) = \text{span } \{\phi_{0k} : \forall k \geq 0\}. \quad (2.10)$$

Dimension matching. We study now the biorthogonality of the generators of $V_0(\mathbb{R}^+)$ and $\tilde{V}_0(\mathbb{R}^+)$, where the dual construction is obtained by following the same guidelines used for the primal one. Setting

$$k^* = \max\{k_0^*, \tilde{k}_0^*\} = \max\{-n_0 + \delta, -\tilde{n}_0 + \tilde{\delta}\},$$

we can observe that $\{\varphi_{0k}^{\mathbb{R}} : k \geq k^*\}$ and $\{\tilde{\varphi}_{0k}^{\mathbb{R}} : k \geq k^*\}$ are already biorthogonal. In order to get a pair of biorthogonal systems, we have therefore to match the dimensions of the spaces spanned by

$$\{\phi_{0\alpha} : \alpha = 0, \dots, L-1\} \cup \{\varphi_{0k}^{\mathbb{R}} : k = k_0^*, \dots, k^* - 1\}$$

and by

$$\{\tilde{\phi}_{0\beta} : \beta = 0, \dots, \tilde{L}-1\} \cup \{\tilde{\varphi}_{0k}^{\mathbb{R}} : k = \tilde{k}_0^*, \dots, k^* - 1\}.$$

This requirement can be translated into an explicit relation between δ and $\tilde{\delta}$; indeed, we must have $L - k_0^* = \tilde{L} - \tilde{k}_0^*$, i.e.,

$$\tilde{\delta} - \delta = \tilde{L} - L + \tilde{n}_0 - n_0. \quad (2.11)$$

Since $\tilde{L} \geq L$, we get $k^* = -\tilde{n}_0 + \tilde{\delta}$. It should be noted that the two parameters δ and $\tilde{\delta}$ have been introduced exactly because we want the equality of the cardinality of the sets previously indicated. On the other hand, we want to choose them as small as possible in order to minimize the perturbation due to the boundary. Thus, it will be natural to fix either δ or $\tilde{\delta}$ equal to zero and determine the other one from the relation (2.11). For systems arising from B-spline functions, it can be seen^{19,12} that, if $\tilde{\delta} = 0$, we have $0 \leq \delta < L$.

Boundary and interior scaling functions. Let us define the spaces V_0^B and \tilde{V}_0^B , spanned by the so called *boundary scaling functions*, as

$$V_0^B := \text{span} \{\phi_{0k} : k = 0, \dots, \tilde{L}-1\}, \quad \tilde{V}_0^B := \text{span} \{\tilde{\phi}_{0k} : k = 0, \dots, \tilde{L}-1\},$$

and the spaces V_0^I and \tilde{V}_0^I spanned by the *interior scaling functions* as

$$V_0^I := \text{span} \{\phi_{0k} : k \geq \tilde{L}\}, \quad \tilde{V}_0^I := \text{span} \{\tilde{\phi}_{0k} : k \geq \tilde{L}\}.$$

We have

$$V_0(\mathbb{R}^+) = V_0^B \oplus V_0^I, \quad \tilde{V}_0(\mathbb{R}^+) = \tilde{V}_0^B \oplus \tilde{V}_0^I. \quad (2.12)$$

Note that, if $L < \tilde{L}$, the subspace V_0^I is strictly contained in $V^{(+)}$ (see (2.10)). In other words, some of the functions in $V^{(+)}$ (which are scaling functions on \mathbb{R} supported in $[0, +\infty)$) are thought as boundary scaling functions, i.e., are included in V_0^B .

Biorthogonality. Recalling that V_0^I is already biorthogonal to \tilde{V}_0^I and that

$$V_0^B \perp \tilde{V}_0^I, \quad V_0^I \perp \tilde{V}_0^B,$$

we only need to modify the border functions in order to obtain fully biorthogonal systems. The problem is then to find a basis of V_0^B , say $\{\varphi_{0k} : k = 0, \dots, \tilde{L}-1\}$, and one of \tilde{V}_0^B , say $\{\tilde{\varphi}_{0l} : l = 0, \dots, \tilde{L}-1\}$, such that

$$\langle \varphi_{0k}, \tilde{\varphi}_{0l} \rangle_{\mathbb{R}^+} := \int_{\mathbb{R}^+} \varphi_{0k}(x) \tilde{\varphi}_{0l}(x) dx = \delta_{kl}, \quad k, l = 0, \dots, \tilde{L}-1.$$

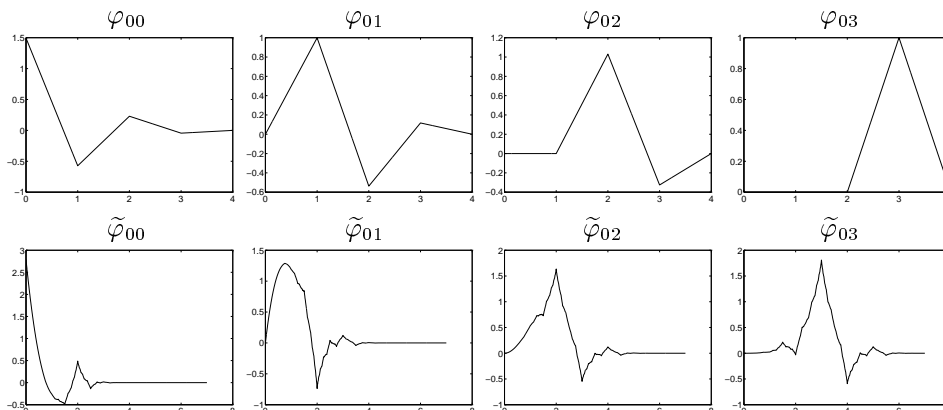


Fig. 1. Primal (top row) and dual (bottom row) border scaling functions obtained from a B-spline multiresolution with $L = 2$ and $\tilde{L} = 4$.

Setting $\varphi_{0k} = \sum_{m=0}^{\tilde{L}-1} D_{km} \phi_{0m}$ and $\tilde{\varphi}_{0k} = \sum_{m=0}^{\tilde{L}-1} \tilde{D}_{km} \tilde{\phi}_{0m}$, and calling \mathbf{X} the Gramian matrix of components

$$X_{kl} = \langle \phi_{0k}, \tilde{\phi}_{0l} \rangle_{\mathbb{R}^+}, \quad k, l = 0, \dots, \tilde{L} - 1,$$

this is equivalent to finding two $\tilde{L} \times \tilde{L}$ real matrices $\mathbf{D} = \{D_{km}\}$ and $\tilde{\mathbf{D}} = \{\tilde{D}_{km}\}$ satisfying

$$\mathbf{D} \mathbf{X} \tilde{\mathbf{D}}^T = \mathbf{I}. \quad (2.13)$$

A necessary and sufficient condition for (2.13) to have solutions is the non-singularity of \mathbf{X} , or equivalently $V_0^B \cap (\tilde{V}_0^B)^\perp = \{0\}$. We know at present of no general result establishing the invertibility of \mathbf{X} , although it can be proved, e.g., for orthogonal systems¹ and for systems arising from B-spline functions.^{19,12} From now on we will assume that this condition is verified. If this is the case, there exist infinitely many couples which satisfy Eq. (2.13). We describe in Section 5 a particular biorthogonalization scheme leading to scaling functions with good localization properties. This is illustrated in the example of Fig. 1, which reports plots of the biorthogonal border scaling functions derived from a B-spline multiresolution with $L = 2$ and $\tilde{L} = 4$.

Renaming now the functions of V_0^I and \tilde{V}_0^I as

$$\varphi_{0k} = \phi_{0k}, \quad \tilde{\varphi}_{0l} = \tilde{\phi}_{0l}, \quad \forall k, l \geq \tilde{L},$$

we can conclude that the two sets $\{\varphi_{0k} : k \geq 0\}$ and $\{\tilde{\varphi}_{0l} : l \geq 0\}$ are dual biorthogonal bases of $V_0(\mathbb{R}^+)$ and $\tilde{V}_0(\mathbb{R}^+)$, respectively. It can be proved that these bases are 2-stable, in the sense that

$$V_0(\mathbb{R}^+) = \left\{ v = \sum_{k \geq 0} \alpha_k \varphi_{0k} : \{\alpha_k\}_{k \in \mathbb{N}} \in \ell^2 \right\}$$

with

$$\|v\|_{L^2(\mathbb{R}^+)} \asymp \|\{\alpha_k\}_{k \in \mathbb{N}}\|_{\ell^2}, \quad \forall v \in V_0(\mathbb{R}^+),$$

and similarly for the dual system.

Refinement equations. Let us introduce the isometries $T_j : L^2(\mathbb{R}^+) \rightarrow L^2(\mathbb{R}^+)$ defined as

$$(T_j f)(x) = 2^{j/2} f(2^j x), \quad (2.14)$$

and set $\varphi_{jk} = T_j \varphi_{0k}$, $\forall j, k \geq 0$. We define the j -th level scaling function spaces as

$$V_j(\mathbb{R}^+) := T_j(V_0(\mathbb{R}^+)).$$

It can be shown that this is a family of refinable spaces, i.e., $V_j(\mathbb{R}^+) \subset V_{j+1}(\mathbb{R}^+)$. This allows to define a *refinement equation*

$$\varphi_{jk} = \sum_{m \geq 0} \mathcal{H}_{km} \varphi_{j+1,m} \quad (2.15)$$

that generalize the corresponding Eq. (2.3) holding for the scaling functions on the real line. Similar observations can be applied for the dual construction. Some important considerations on these filter matrices will be found in Section 2.3.

Projection operators. Once a pair of biorthogonal generators φ_{jk} and $\tilde{\varphi}_{jk}$ has been defined, it is possible to consider suitable projection operators $P_j : L^2(\mathbb{R}^+) \rightarrow V_j(\mathbb{R}^+)$, defined as

$$P_j v = \sum_{k \geq 0} \check{v}_{jk} \varphi_{jk}, \quad \text{with } \check{v}_{jk} := \langle v, \tilde{\varphi}_{jk} \rangle_{\mathbb{R}^+}. \quad (2.16)$$

One can prove that they are well defined, continuous, and uniformly bounded. In addition, we have that $P_j v = v$, $\forall v \in V_j(\mathbb{R}^+)$ and $P_j \circ P_{j+1} = P_j$. Similar relations hold for the dual system. These operators will be used in Section 3 to define appropriate wavelet bases.

2.3. On the border scaling function filters

The structure of the matrix \mathcal{H} in the refinement equation (2.15) and of its dual counterpart $\tilde{\mathcal{H}}$ is important for the applications, because the computational efficiency of wavelet-based algorithms strongly depends on the length of the filters. Therefore, it is fundamental to keep the structure of these matrices as sparse as possible. Figure 2 reports the position of the nonzero entries in the filter matrices corresponding to the example of Fig. 1. For illustration purposes the matrices have been truncated and only the upper-left blocks are displayed. It should be noted that starting from row \tilde{L} (recall that indexing starts from 0 and $\tilde{L} = 4$) the matrix entries refer to functions of the internal spaces, which can be expressed in terms of the internal functions at the next refinement level. Therefore, the rows of the filter

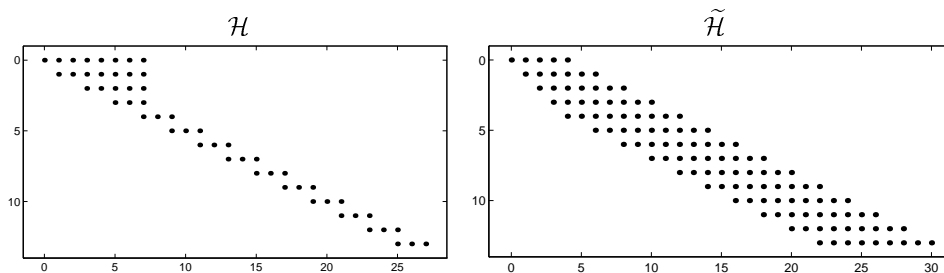


Fig. 2. Structure of the filter matrices \mathcal{H} and $\tilde{\mathcal{H}}$ for the scaling functions obtained from a B-spline multiresolution with $L = 2$ and $\tilde{L} = 4$. Each dot represents a nonzero entry.

matrices starting from row \tilde{L} are formed by translations of the filters h and \tilde{h} , as indicated by Eq. (2.3) and by its dual counterpart. Precisely, we have

$$\mathcal{H}_{km} = h_{m-k^*+\tilde{L}-2k}, \quad \forall k \geq \tilde{L}, \quad (2.17)$$

and similarly for the dual filters. On the other hand, the rows $0, \dots, \tilde{L} - 1$ refer to the border scaling functions, which are expressed in terms of both border functions and internal functions at the next refinement level. However, the number of involved internal functions remains small, as well as the length of the modified border filters. More precisely, the number of nonzero entries in the first \tilde{L} rows can be explicitly calculated, obtaining

$$\mathcal{H}_{km} = 0, \quad \forall m \geq N_h \quad \text{and} \quad \tilde{\mathcal{H}}_{km} = 0, \quad \forall m \geq N_{\tilde{h}}, \quad \forall k = 0, \dots, \tilde{L} - 1,$$

where

$$N_h = \tilde{L} + k^* + n_1 - 1, \quad N_{\tilde{h}} = \tilde{L} + k^* + \tilde{n}_1 - 1. \quad (2.18)$$

We want to point out (see again Fig. 2) that in our construction the upper-left blocks are upper-triangular. This is possible through the biorthogonalization scheme described in Section 5, which produces both well localized scaling functions (see Fig. 1) and short border filters.

3. Wavelet Spaces for the Half-Line

In this section we construct the wavelets and the detail spaces on the half-line. We will partly follow Refs. 19 and 3, but we propose a new definition of “border wavelets” (see Eq. (3.3)) which seems to be more suitable for the applications. Specifically, the new definition will lead to short border wavelet filters and to well localized border wavelets when used in conjunction with the triangular biorthogonalization scheme described in Section 5.

Interaction with the border. We start from level $j = 0$ and look for a complement space $W_0(\mathbb{R}^+)$ such that $V_1(\mathbb{R}^+) = V_0(\mathbb{R}^+) \oplus W_0(\mathbb{R}^+)$ (note that the sum is

not, in general, orthogonal) and $W_0(\mathbb{R}^+) \perp \tilde{V}_0(\mathbb{R}^+)$. To this end, we consider the basis functions of $V_1(\mathbb{R}^+)$ and write them as a sum of an element in $V_0(\mathbb{R}^+)$ and a function which will be an element of $W_0(\mathbb{R}^+)$. As for the scaling functions, we need to distinguish between internal wavelets, which are inherited from the decomposition on \mathbb{R} and which will not be modified, and border wavelets, which need to be explicitly defined.

Interior wavelets. Since $V_0(\mathbb{R}^+)$ contains the subspace $V^{(+)}$ defined in (2.7), $V_1(\mathbb{R}^+)$ contains the subspace $V_1^{(+)} = T_1 V^{(+)} = \{\varphi_{1k}^{\mathbb{R}}|_{[0,+\infty)} : k \geq k_0^*\}$. Considering Eq. (2.4), it is possible to identify which wavelets can be reconstructed by using only scaling functions in $V_1^{(+)}$. This corresponds to finding a lower bound on m in Eq. (2.4), such that all the indices k in the sum are greater than or equal to k_0^* . This is equivalent to $2m \geq k_0^* + \tilde{n}_1 - 1$, so we set

$$m \geq \lceil \frac{k_0^* + \tilde{n}_1 - 1}{2} \rceil =: m_0^*$$

(where $\lceil x \rceil$ indicates the smallest integer greater than or equal to x). Let us set

$$W_0^{(+)} := \text{span} \{ \psi_{0m}^{\mathbb{R}}|_{[0,+\infty)} : m \geq m_0^* \};$$

we observe that $W_0^{(+)}$ can be identified with a subspace of $W_0(\mathbb{R})$ generated by wavelets supported in $[0, +\infty)$, so it is orthogonal to $\tilde{V}_0(\mathbb{R}^+)$ and $W_0^{(+)} \subseteq W_0(\mathbb{R}^+)$. Let W_0^A be a generic supplementary space of $W_0^{(+)}$ in $W_0(\mathbb{R}^+)$. It can be easily proved that $\dim W_0^A = m_0^*$. Therefore, we need to define additional m_0^* functions that, together with the basis functions of $W_0^{(+)}$ and $V_0(\mathbb{R}^+)$, will generate $V_1(\mathbb{R}^+)$.

Border wavelets. Let us first identify which functions of $V_1(\mathbb{R}^+)$ we are able to generate with the internal scaling function and wavelet spaces only. These spaces are generated by $\{\varphi_{0m}^{\mathbb{R}}|_{[0,+\infty)}, m \geq k_0^*\}$ and $\{\psi_{0m}^{\mathbb{R}}|_{[0,+\infty)}, m \geq m_0^*\}$, respectively. Substituting these functions in Eq. (2.5) and enforcing the bounds on m , we get a lower bound on k . More precisely, the internal spaces generate the functions $\{\varphi_{1k}^{\mathbb{R}}|_{[0,+\infty)}, k \geq \bar{k}\}$, with

$$\bar{k} = 2k_0^* + \tilde{n}_1 - 1.$$

It was proved¹⁹ that the remaining functions of $V_1(\mathbb{R}^+)$ can be generated by adding the border wavelets defined as

$$\xi_{0m} := (\text{Id} - P_0)\varphi_{1,k_m}^{\mathbb{R}}|_{[0,+\infty)}, \quad m = 0, \dots, m_0^* - 1, \quad (3.1)$$

where P_0 is the projection operator defined in Eq. (2.16) and $k_m = \bar{k} + 2m - 2m_0^* + 1$. Therefore, setting

$$W_0^A = \{\xi_{0m} : m = 0, \dots, m_0^* - 1\},$$

we can define the wavelet space as

$$W_0(\mathbb{R}^+) = W_0^A \oplus W_0^{(+)},$$

so that

$$V_1(\mathbb{R}^+) = V_0(\mathbb{R}^+) \oplus W_0(\mathbb{R}^+).$$

The same procedure leads to the construction of the dual wavelet space $\widetilde{W}_0(\mathbb{R}^+)$.

As for the scaling functions, we must find a couple of biorthogonal bases for the spaces $W_0(\mathbb{R}^+)$ and $\widetilde{W}_0(\mathbb{R}^+)$. Setting

$$m^* = \max\{m_0^*, \widetilde{m}_0^*\},$$

we can define, in analogy with the procedure followed for the definition of the scaling function spaces, the *internal* and *border wavelet spaces*, respectively, as

$$W_0^B := \text{span} \{\xi_{0m} : m = 0, \dots, m^* - 1\}, \quad W_0^I := \text{span} \{\psi_{0m} : m \geq m^*\}, \quad (3.2)$$

where we have set $\xi_{0m} := \psi_{0m}^{\mathbb{R}}|_{[0,+\infty)}$ if $m_0^* \leq m < m^*$ and $\psi_{0m} := \psi_{0m}^{\mathbb{R}}|_{[0,+\infty)}$ if $m \geq m^*$. The dual spaces are defined accordingly. From the properties of the construction on the real line, we have that W_0^I and \widetilde{W}_0^I are biorthogonal, i.e.,

$$\langle \psi_{0m}, \widetilde{\psi}_{0n} \rangle_{\mathbb{R}^+} = \delta_{mn}, \quad \forall m, n \geq m^*.$$

Note, however, that the biorthogonality between the internal and the border wavelet spaces is not guaranteed. Therefore, any biorthogonalization applied to the border wavelets only (as we did for the scaling functions) would not lead to fully biorthogonal wavelet spaces. This problem can be solved¹⁹ by adding a suitable number of primal and dual internal wavelets to the border wavelet spaces, and by performing the biorthogonalization on this enlarged set. However, this procedure leads to a large number of border wavelets. In addition, the modified border wavelet filters result quite long if compared to the filters of the internal wavelets. These two facts contraddict the main philosophy of the construction, which should be founded on the smallest number of modifications with respect to the multiresolution on \mathbb{R} in order to account for the border $x = 0$. For this reason, we suggest an alternative definition of the border wavelets with respect to Eq. (3.1). These new wavelets will be automatically biorthogonal to the internal wavelets, and will be characterized by much shorter filters with respect to other constructions.^{12,19,20}

Improved definition for border wavelets. The proposed new definition of the border wavelets is

$$\xi_{0m} := (\text{Id} - P_0 - Q_0^I)\varphi_{1,k_m}^{\mathbb{R}}|_{[0,+\infty)}, \quad m = 0, \dots, m_0^* - 1, \quad (3.3)$$

where Q_0^I is a projection operator onto the internal wavelet spaces, defined, $\forall v \in L^2(\mathbb{R}^+)$, as

$$Q_0^I v = \sum_{m \geq m^*} \hat{v}_{0m} \psi_{0m}, \quad \text{with} \quad \hat{v}_{0m} := \langle v, \widetilde{\psi}_{0m} \rangle_{\mathbb{R}^+}.$$

Using a similar definition for the dual wavelets, it is clear that the following relations hold,

$$W_0^B \perp \widetilde{W}_0^I, \quad W_0^I \perp \widetilde{W}_0^B,$$

while the interior wavelets spaces W_0^I and \widetilde{W}_0^I are already biorthogonal. Consequently, only the biorthogonality between the primal and dual border wavelets needs to be enforced. We can follow the same procedure as used for the scaling functions, i.e., find a basis of W_0^B , say $\{\psi_{0m} : m = 0, \dots, m^* - 1\}$, and one of \widetilde{W}_0^B , say $\{\tilde{\psi}_{0n} : n = 0, \dots, m^* - 1\}$, such that

$$\langle \psi_{0m}, \tilde{\psi}_{0n} \rangle_{\mathbb{R}^+} = \delta_{mn}, \quad m, n = 0, \dots, m^* - 1.$$

Setting $\psi_{0m} = \sum_{k=0}^{m^*-1} E_{mk} \xi_{0k}$ and $\tilde{\psi}_{0n} = \sum_{l=0}^{m^*-1} \tilde{E}_{nl} \tilde{\xi}_{0l}$, and denoting by \mathbf{Y} the Gramian matrix of components

$$Y_{kl} = \langle \xi_{0k}, \tilde{\xi}_{0l} \rangle_{\mathbb{R}^+}, \quad k, l = 0, \dots, m^* - 1,$$

this is equivalent to finding two $m^* \times m^*$ real matrices \mathbf{E} and $\tilde{\mathbf{E}}$ satisfying

$$\mathbf{E} \mathbf{Y} \tilde{\mathbf{E}}^T = \mathbf{I}. \quad (3.4)$$

It is not difficult to see³ that the invertibility of \mathbf{Y} follows from the invertibility of \mathbf{X} . Therefore, this problem is identical to Eq. (2.13), and will not be further discussed here. Additional considerations can be found in Section 5. In summary, we have constructed two sets of biorthogonal generators for the wavelet spaces, which we will indicate as

$$W_0(\mathbb{R}^+) = \text{span} \{\psi_{0m} : m \geq 0\} \quad \text{and} \quad \widetilde{W}_0(\mathbb{R}^+) = \text{span} \{\tilde{\psi}_{0m} : m \geq 0\}.$$

Refinement equations. Using now the isometries (2.14), we set $\psi_{jm} = T_j \psi_{0m}$, $\forall j, m \geq 0$. Accordingly, we define the j -th level wavelet spaces as

$$W_j(\mathbb{R}^+) := T_j(W_0(\mathbb{R}^+)).$$

Clearly, these are included in the scaling function spaces at the next refinement level,

$$W_j(\mathbb{R}^+) \subset V_{j+1}(\mathbb{R}^+).$$

This allows to define a wavelet *refinement equation*

$$\psi_{jk} = \sum_{m \geq 0} \mathcal{G}_{km} \varphi_{j+1, m},$$

that generalizes the corresponding Eq. (2.4) holding for the wavelets on the real line. Similar considerations hold for the dual setting.

Wavelet filters. We focus now on the wavelet filters, giving some additional details about their construction. The following calculations will show that the length of the

border wavelet filters is limited by the length of the border scaling function filters. Without loss of generality, we will discuss the case $m_0^* \geq \tilde{m}_0^*$, which is compatible with the assumption $L \leq \tilde{L}$ or, equivalently, $k_0^* \leq \tilde{k}_0^*$. Otherwise, the role of primal and dual functions can be exchanged. In what follows, we will set $m < m_0^*$ for the primal wavelets and $m < \tilde{m}_0^*$ for the dual wavelets.

Recalling the definition (3.3), we need to compute the projection of a scaling function $\varphi_{1k}^{\mathbb{R}}$ onto the scaling function space and the internal wavelet space. A straightforward calculation leads to the expressions

$$P_0 \varphi_{1k}^{\mathbb{R}} = \sum_{l \geq 0} \Pi_{kl} \varphi_{0l}, \quad \tilde{P}_0 \tilde{\varphi}_{1k}^{\mathbb{R}} = \sum_{l \geq 0} \tilde{\Pi}_{kl} \tilde{\varphi}_{0l},$$

where

$$\begin{aligned} \Pi_{kl} &= \begin{cases} \sum_{n=0}^{\tilde{L}-1} [\mathbf{D}^{-1}]_{L+k-k_0^*, n} \tilde{\mathcal{H}}_{ln} & \text{if } k_0^* \leq k < k^*, \\ \tilde{\mathcal{H}}_{l, \tilde{L}+k-k^*} & \text{if } k \geq k^*, \end{cases} \\ \tilde{\Pi}_{kl} &= \langle \tilde{\varphi}_{1k}^{\mathbb{R}}, \varphi_{0l} \rangle_{\mathbb{R}^+} = \mathcal{H}_{l, \tilde{L}+k-k^*}, \quad k \geq k^*, \end{aligned} \quad (3.5)$$

and to

$$Q_0^I \varphi_{1k}^{\mathbb{R}} = \sum_{n \geq m^*} \tilde{g}_{k-2n} \psi_{0n}, \quad \tilde{Q}_0^I \tilde{\varphi}_{1k}^{\mathbb{R}} = \sum_{n \geq m^*} g_{k-2n} \tilde{\psi}_{0n}.$$

Substituting now in Eq. (3.3), and using Eq. (2.15) with their dual counterpart, we obtain the refinement equations for the non-biorthogonal border wavelets,

$$\xi_{0m} = \sum_{l \geq 0} G_{ml} \varphi_{1l}, \quad \tilde{\xi}_{0m} = \sum_{l \geq 0} \tilde{G}_{ml} \tilde{\varphi}_{1l}. \quad (3.6)$$

The complete expression of G and \tilde{G} can be easily obtained through straightforward substitutions and will not be reported here. Rather, we proceed to explicitly computing the length of the border filters. For this reason, we focus on the cases $l \geq \tilde{L}$ and m such that $k_m, \tilde{k}_m \geq k^*$. The first bound allows to individuate which internal scaling functions are involved in the refinement equations (obviously, it is clear that the border scaling functions will always be involved). The second bound allows to simplify the expressions of the wavelet filters, because under this limitation only the second row in Eq. (3.5) is needed for the calculations. Again, this only affects the border scaling functions. A straightforward calculation leads to the expressions

$$\begin{aligned} G_{ml} &= \delta_{k_m - k^* + \tilde{L}, l} - \sum_{n \geq 0} \tilde{\mathcal{H}}_{n, \tilde{L}+k_m - k^*} \mathcal{H}_{nl} - \sum_{n \geq m^*} \tilde{g}_{k_m - 2n} g_{k^* + l - \tilde{L} - 2n}, \\ \tilde{G}_{ml} &= \delta_{\tilde{k}_m - k^* + \tilde{L}, l} - \sum_{n \geq 0} \mathcal{H}_{n, \tilde{L} + \tilde{k}_m - k^*} \tilde{\mathcal{H}}_{nl} - \sum_{n \geq m^*} g_{\tilde{k}_m - 2n} \tilde{g}_{k^* + l - \tilde{L} - 2n}. \end{aligned}$$

Substituting now the expression (2.17) for the scaling function filters and using the

identity (2.6), we obtain

$$\begin{aligned}
G_{ml} &= - \sum_{n=0}^{\tilde{L}-1} \tilde{\mathcal{H}}_{n, \tilde{L}+k_m-k^*} \mathcal{H}_{nl} + \\
&\quad + \sum_{n \leq k^*-1} \tilde{h}_{k_m-2n} h_{k^*+l-\tilde{L}-2n} + \sum_{n \leq m^*-1} \tilde{g}_{k_m-2n} g_{k^*+l-\tilde{L}-2n}, \\
\tilde{G}_{ml} &= - \sum_{n=0}^{\tilde{L}-1} \mathcal{H}_{n, \tilde{L}+\tilde{k}_m-k^*} \tilde{\mathcal{H}}_{nl} + \\
&\quad + \sum_{n \leq k^*-1} h_{\tilde{k}_m-2n} \tilde{h}_{k^*+l-\tilde{L}-2n} + \sum_{n \leq m^*-1} g_{\tilde{k}_m-2n} \tilde{g}_{k^*+l-\tilde{L}-2n}.
\end{aligned}$$

These expressions are convenient because of the explicit upper limits in the summations. They allow to calculate the number of nonvanishing entries in each row of G and \tilde{G} . More precisely, it is easy to show that

$$\begin{aligned}
G_{ml} &= 0 && \text{if } l \geq N_g \\
\tilde{G}_{ml} &= 0 && \text{if } l \geq N_{\tilde{g}},
\end{aligned}$$

where

$$\begin{aligned}
N_g &= \max\{N_h, L + \tilde{n}_1 - \tilde{n}_0 - 1 + \nu\}, \\
N_{\tilde{g}} &= \max\{N_{\tilde{h}}, \tilde{L} + \tilde{n}_1 - n_0 - 1 + \nu\},
\end{aligned}$$

and $\nu = \delta \bmod 2$. Moreover, recalling definition (2.18), $N_g \leq N_{\tilde{h}} + 1$, with the equality holding only when $L = \tilde{L}$ and δ odd, and $N_{\tilde{g}} = N_{\tilde{h}}$. Thus, the length of the border wavelet filters is essentially limited by the length of the border scaling function filters. This was not true for the previous construction,¹⁹ where the wavelet filters could be long even as twice as the scaling function filters. Finally, the biorthogonal filters \tilde{G} and $\tilde{\mathcal{G}}$ are easily found by applying the change of basis through matrices \mathbf{E} and $\tilde{\mathbf{E}}$ to Eqs. (3.6).

Examples. We conclude this section by showing plots of the border wavelets (Fig. 3) in the B-spline case with $L = 2$ and $\tilde{L} = 4$ (see also Fig. 1). Note the good localization of each border wavelet ψ_{0m} , $\tilde{\psi}_{0m}$ around the dyadic points $(2m+1)2^{-1}$, due to the optimal biorthogonalization performed according to the guidelines in Section 5. Note that it is also possible to modify the single nonvanishing primal and dual wavelets ψ_{00} and $\tilde{\psi}_{00}$ so that their value at $x = 0$ is the same as the corresponding scaling functions. This can be accomplished by a simple renormalization through a constant, because it can be shown⁴ that $\varphi_{00}(0)\tilde{\varphi}_{00}(0) = \psi_{00}(0)\tilde{\psi}_{00}(0)$. A similar normalization is usually referred as *boundary adaption*, and proves quite useful in applications based on domain decompositions for the solution of PDE's.⁵ Figure 4 depicts the structure of the biorthogonal wavelet filters, which is similar

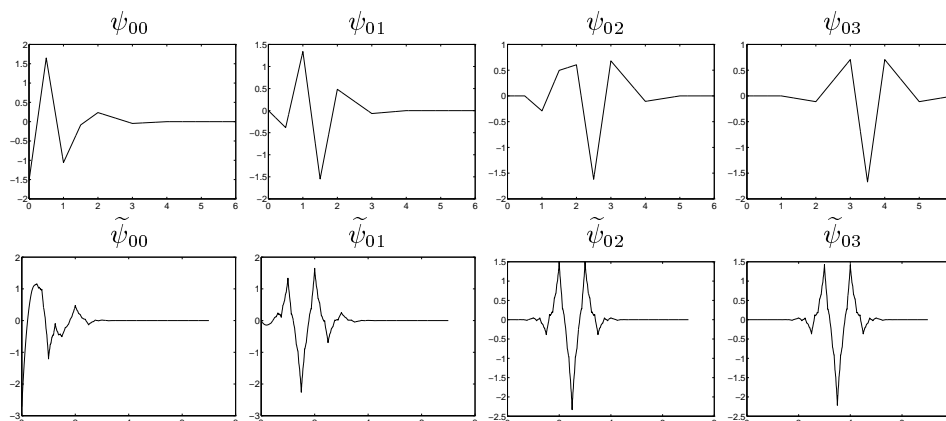


Fig. 3. Primal (top row) and dual (bottom row) border wavelets obtained from a B-spline multiresolution with $L = 2$ and $\tilde{L} = 4$.

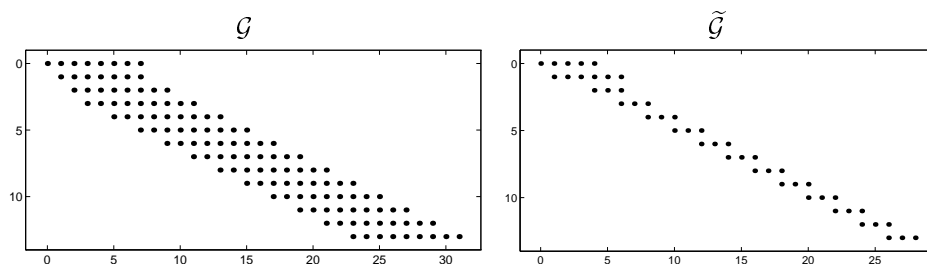


Fig. 4. Structure of the filter matrices \mathcal{G} and $\tilde{\mathcal{G}}$ for the wavelets obtained from a B-spline multiresolution with $L = 2$ and $\tilde{L} = 4$. Each dot represents a nonzero entry.

to the scaling function filters. In particular, the upper-left blocks corresponding to the border wavelets are characterized by a small number of nonvanishing entries.

4. The Unit Interval

This section describes how the multilevel decomposition of the half-line derived in the previous sections can be adapted to build a multilevel decomposition of the unit interval $I = (0, 1)$. The main point is to merge two parallel decompositions on the half-lines $(0, +\infty)$ and $(-\infty, 1)$ obtained from the same decomposition on \mathbb{R} . This procedure requires that the effects of the two boundary points $x = 0$ and $x = 1$ can be treated independently. We will see that this imposes a lower bound on the refinement level j used in the decomposition.

The construction on $(0, +\infty)$ has been described above. To obtain the decomposition on $(-\infty, 1)$, it is natural to consider the one on $(-\infty, 0)$ and shift it rightwards by 1. The construction on $(-\infty, 0)$ is achieved by repeating the adaption of scaling functions and wavelets on \mathbb{R} to the boundary point for $x \leq 0$. We do not report

here the details, which follow the same guidelines of Sections 2 and 3.

The structure of the scaling function and wavelet spaces on the unit interval will be

$$\begin{aligned} V_j(0,1) &= \text{span} \{ \varphi_{jl}^{(0)} : l \in \mathcal{I}_L \} \oplus \\ &\quad \text{span} \{ \varphi_{jk} : k \in \mathcal{I}_I \} \oplus \\ &\quad \text{span} \{ \varphi_{jr}^{(1)} : r \in \mathcal{I}_R \}, \quad \forall j \geq j_0, \\ W_j(0,1) &= \text{span} \{ \psi_{jl}^{(0)} : l \in \mathcal{K}_L \} \oplus \\ &\quad \text{span} \{ \psi_{jk} : k \in \mathcal{K}_I \} \oplus \\ &\quad \text{span} \{ \psi_{jr}^{(1)} : r \in \mathcal{K}_R \}, \quad \forall j \geq j_0, \end{aligned}$$

where the suffixes ⁽⁰⁾ or ⁽¹⁾ label those scaling functions and wavelets that have been redefined to account for the boundary points $x = 0$ and $x = 1$, respectively, and where \mathcal{I}_L , \mathcal{I}_I , \mathcal{I}_R , \mathcal{K}_L , \mathcal{K}_I , and \mathcal{K}_R indicate suitable sets of indices. In order to decouple the effects of the two boundary points, there must be at least one internal scaling function, i.e., $\mathcal{I}_I \neq \emptyset$. This can be identified with a scaling function in each decomposition on $(0, +\infty)$ and $(-\infty, 1)$. These in turn can be both identified with the same scaling function of the underlying decomposition on \mathbb{R} . Obviously, its support must be strictly included in $(0, 1)$. The same considerations apply for the wavelets, leading to $\mathcal{K}_I \neq \emptyset$. As the supports of scaling functions and wavelets on \mathbb{R} at level j have length proportional to 2^{-j} , there must be a minimum level j_0 such that $\forall j \geq j_0$ the above decoupling conditions are verified.

In the particular case of scaling functions and wavelets characterized by central symmetry, like the systems arising from B-spline functions, it is easy to show that the whole construction on $(-\infty, 0)$ can be derived from the construction on $(0, +\infty)$ through reflection around the origin. Therefore, all the border functions at the right boundary can be derived from the border functions at the left boundary by reflection and translation by 1, as depicted in Fig. 5.

5. Biorthogonalization

In this section we describe the biorthogonalization process used for the construction of the border scaling functions and wavelets. Some considerations are in order to introduce the motivations underlying the proposed biorthogonalization scheme, which is detailed in the first subsection. In fact, the solution to Equations (2.13) and (3.4) is obviously not unique. Therefore, we need some criteria for the determination of a particular solution that enhances those features that are useful for the applications. Our choice will be to preserve as much as possible the localization of the border scaling functions and wavelets. This is indeed a fundamental requirement for those applications based on adaptive representations obtained through nonlinear wavelet approximations^{4,17,18} (see the example reported in the forthcoming section).

Let us recall the decomposition of the scaling functions and wavelets spaces into “internal” and “border” subspaces (Eqs. (2.12) and (3.2)). The internal spaces are

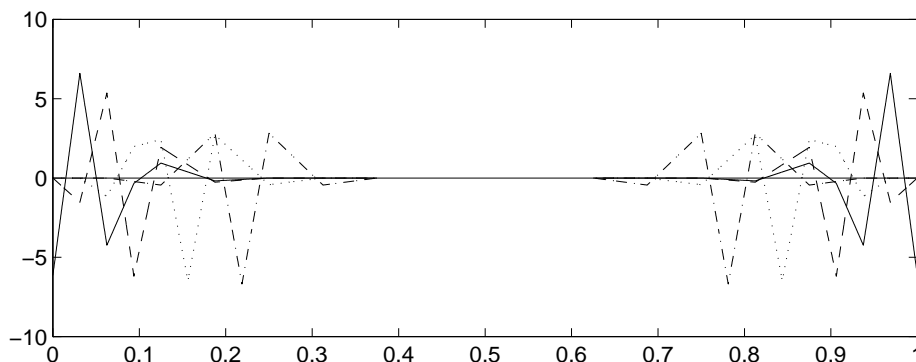


Fig. 5. Primal border wavelets on the unit interval constructed from a B-spline multiresolution with $L = 2$ and $\tilde{L} = 4$. The refinement level is $j = 4$.

generated by the same scaling functions and wavelets defined on the real line. The latter are compactly supported and therefore well localized. On the other hand, the border scaling functions and wavelets defined in Eqs. (2.9) and (3.3) are expressed as linear combinations of the corresponding functions defined on the real line. From these expressions we see that all the border scaling functions and wavelets have the same support. Therefore, they lead to a worse localization with respect to the internal functions. These considerations suggest to improve the localization of the biorthogonal border scaling functions and wavelets by using the additional degrees of freedom intrinsic in the biorthogonalization process. In particular, we want to insure that each border wavelet ψ_{jk} has most of its energy concentrated around the point $x_{jk} = (2k + 1)2^{-j-1}$ of a dyadic grid. This property holds for the wavelets of the decomposition on \mathbb{R} , but it can be lost in the definition of the border functions of Eq. (3.3). Also, previous constructions of wavelets on the unit interval led to poorly localized border wavelets.^{12,13,20}

We have seen in Section 2.2 that the border scaling functions are constructed by imposing the reconstruction of all polynomials of a certain degree. A set of basis functions $\{p_\alpha : \alpha = 0, \dots, L-1\}$ for the space of polynomials \mathcal{P}_{L-1} (and similarly for the dual system) must be chosen to proceed with the construction. We will see that well localized border scaling functions and wavelets can be obtained when these basis polynomials are such that

$$p_\alpha(x) = x^\alpha q_\alpha(x), \quad \forall \alpha = 0, \dots, L-1, \quad (5.1)$$

where $q_\alpha(x)$, $\forall \alpha = 0, \dots, L-1$ is a polynomial that does not vanish at $x = 0$. The basis of monomials obviously satisfies this property. However, it was shown¹² that this basis leads to an ill-conditioned Gramian matrix \mathbf{X} . Other bases, like, e.g., the Bernstein polynomials, still satisfy Eq. (5.1) and lead to Gramian matrices with better condition numbers.^{13,20} If Eq. (5.1) is satisfied, the non-biorthogonal border scaling functions $\phi_{0\alpha}$ (and similarly for the duals) have a zero of order α

at $x = 0$. If this property is preserved by the biorthogonal scaling functions, these will be localized around a center that shifts towards right for increasing values of α (see the example reported in Fig. 1). This can be accomplished by forcing the structure of the change of basis matrices \mathbf{D} and $\tilde{\mathbf{D}}$ to be upper-triangular. It is straightforward to verify that also the biorthogonal scaling functions filters \mathcal{H} , $\tilde{\mathcal{H}}$ result upper-triangular.

A similar consideration can be applied to the wavelet functions. The definition (3.3) leads to non-biorthogonal wavelets which are not necessarily adapted to the boundary and well localized. In particular, the non-biorthogonal wavelet filters are not upper-triangular. However, a Gaussian elimination can be performed on the rows in the filter matrices corresponding to the border wavelets, to get upper-triangular filters. If a biorthogonalization with upper-triangular matrices \mathbf{E} , $\tilde{\mathbf{E}}$ is performed, also the biorthogonal wavelets filters \mathcal{G} , $\tilde{\mathcal{G}}$ will be upper-triangular, and the corresponding border wavelets ψ_{0k} , $\tilde{\psi}_{0k}$ will have a zero of order k at $x = 0$. The examples of Fig. 5 show that this leads to well-localized primal and dual border wavelets.

In summary, a suitable choice of polynomial bases together with a biorthogonalization performed through upper-triangular matrices for both scaling functions and wavelets leads to well localized hierarchical basis functions. Next subsection describes in detail the proposed algorithm for the triangular biorthogonalization.

5.1. *Triangular biorthogonalization*

As the following applies to both scaling functions and wavelets, we will restate the problem in a general setting by using a common notation. In particular, we will denote the given primal and dual non-biorthogonal basis functions by $\{\theta_k : k = 0, \dots, N-1\}$, $\{\tilde{\theta}_k : k = 0, \dots, N-1\}$, and the primal and dual biorthogonal basis functions, to be determined, by $\{\eta_k : k = 0, \dots, N-1\}$, $\{\tilde{\eta}_k : k = 0, \dots, N-1\}$. These basis functions are related to each other through the $N \times N$ matrices $\mathbf{A} = \{A_{mk}\}$, $\tilde{\mathbf{A}} = \{\tilde{A}_{nl}\}$,

$$\eta_m = \sum_{k=0}^{N-1} A_{mk} \theta_k, \quad \tilde{\eta}_n = \sum_{l=0}^{N-1} \tilde{A}_{nl} \tilde{\theta}_l.$$

The full biorthogonality, i.e. $\langle \eta_k, \tilde{\eta}_l \rangle := \langle \eta_k, \tilde{\eta}_l \rangle_{\mathbb{R}^+} = \delta_{kl}$, can be obtained by finding two upper-triangular real matrices \mathbf{A} and $\tilde{\mathbf{A}}$ satisfying the relation

$$\mathbf{A} \tilde{\mathbf{A}}^T = \mathbf{I}_N, \quad (5.2)$$

where \mathbf{I}_N is the $N \times N$ identity matrix and $\Theta = \{\Theta_{kl}\}$ is the Gramian matrix corresponding to the inner products

$$\Theta_{kl} = \langle \theta_k, \tilde{\theta}_l \rangle, \quad k, l = 0, \dots, N-1.$$

We will assume without further discussion the invertibility of Θ , so that the existence of a solution for Eq. (5.2) is insured.

The first step for the determination of \mathbf{A} , $\tilde{\mathbf{A}}$ is the biorthogonalization of the two functions θ_{N-1} , $\tilde{\theta}_{N-1}$. This consists simply of a renormalization through multiplication by a constant. The biorthogonalization of the remaining functions is obtained by the following iterative scheme.

Let us fix an integer i such that $0 < i < N - 2$ and assume that the sets

$$\mathcal{S}_{i+1} = \{\eta_k : k = i + 1, \dots, N - 1\}, \quad \tilde{\mathcal{S}}_{i+1} = \{\tilde{\eta}_k : k = i + 1, \dots, N - 1\}$$

have already been constructed so that \mathcal{S}_{i+1} is biorthogonal to $\tilde{\mathcal{S}}_{i+1}$. This implies that all the entries $\{A_{mk} : m > i, k \geq m\}$ and $\{\tilde{A}_{nl} : n > i, l \geq n\}$ have already been determined. We want to add the functions η_i and $\tilde{\eta}_i$ to form the sets

$$\mathcal{S}_i = \{\eta_i, \mathcal{S}_{i+1}\}, \quad \tilde{\mathcal{S}}_i = \{\tilde{\eta}_i, \tilde{\mathcal{S}}_{i+1}\}$$

so that \mathcal{S}_i is biorthogonal to $\tilde{\mathcal{S}}_i$. The iteration of this procedure for all values of i ranging from $N - 2$ down to 0 solves the biorthogonalization problem.

Let us write the biorthogonality of \mathcal{S}_i and $\tilde{\mathcal{S}}_i$ in terms of the single elements of the two sets,

$$\langle \eta_i, \tilde{\eta}_i \rangle = 1, \quad \text{and} \quad \langle \eta_i, \tilde{\eta}_s \rangle = 0, \quad \langle \eta_s, \tilde{\eta}_i \rangle = 0, \quad \forall s > i. \quad (5.3)$$

The functions to be added can be expressed as

$$\eta_i = \alpha_i \theta_i + \sum_{s=i+1}^{N-1} \alpha_s \eta_s, \quad \tilde{\eta}_i = \beta_i \tilde{\theta}_i + \sum_{s=i+1}^{N-1} \beta_s \tilde{\eta}_s. \quad (5.4)$$

The linear independence is obviously preserved if the coefficients α_i and β_i are nonvanishing. Substituting now Eq. (5.4) into Eq. (5.3) we get

$$\alpha_s = -\alpha_i \langle \theta_i, \tilde{\eta}_s \rangle, \quad \beta_s = -\beta_i \langle \tilde{\theta}_i, \eta_s \rangle, \quad \forall s > i,$$

and

$$\alpha_i \beta_i K_i = 1, \quad (5.5)$$

where

$$K_i = \langle \theta_i, \tilde{\theta}_i \rangle - \sum_{s=i+1}^{N-1} \langle \theta_i, \tilde{\eta}_s \rangle \langle \tilde{\theta}_i, \eta_s \rangle.$$

Let us now partition the Gramian matrix as

$$\Theta = \begin{bmatrix} \ddots & & & \\ & \Theta_{ii} & \Theta_i^r & \\ & \Theta_i^c & \Theta_{i+1}^o & \\ & & & \ddots \end{bmatrix}$$

and the change of basis matrices as

$$\mathbf{A} = \begin{bmatrix} \ddots & & & \\ & A_{ii} & \mathbf{A}_i^r & \\ & \mathbf{0} & \mathbf{A}_{i+1}^o & \\ & & & \ddots \end{bmatrix}, \quad \tilde{\mathbf{A}} = \begin{bmatrix} \ddots & & & \\ & \tilde{A}_{ii} & \tilde{\mathbf{A}}_i^r & \\ & \mathbf{0} & \tilde{\mathbf{A}}_{i+1}^o & \\ & & & \ddots \end{bmatrix}.$$

Table 1. B-splines (2,4)

δ	N^b	$N^{1/2}$	$N^{1/3}$	$\ e^b\ $	$\ e^{1/2}\ $	$\ e^{1/3}\ $
1×10^{-3}	31	33	31	2.42×10^{-3}	2.14×10^{-3}	1.84×10^{-3}
5×10^{-4}	37	37	34	1.01×10^{-3}	9.31×10^{-4}	1.00×10^{-3}
2×10^{-4}	39	41	37	7.41×10^{-4}	6.75×10^{-4}	6.49×10^{-4}
1×10^{-4}	43	43	37	6.22×10^{-4}	6.27×10^{-4}	6.49×10^{-4}
1×10^{-5}	45	45	46	6.22×10^{-4}	6.26×10^{-4}	6.25×10^{-4}
1×10^{-6}	49	49	51	6.21×10^{-4}	6.25×10^{-4}	6.25×10^{-4}
1×10^{-7}	55	55	57	6.21×10^{-4}	6.25×10^{-4}	6.25×10^{-4}
0	1025	1025	1025	6.21×10^{-4}	6.25×10^{-4}	6.25×10^{-4}

If we define the arrays

$$\boldsymbol{\alpha}_{i+1} = (\alpha_{i+1}, \dots, \alpha_{N-1})^T, \quad \boldsymbol{\beta}_{i+1} = (\beta_{i+1}, \dots, \beta_{N-1})^T,$$

we can express the solution in a more compact matrix form through the following expressions

$$\begin{aligned} K_i &= \Theta_{ii} - \Theta_i^r \left(\tilde{\mathbf{A}}_{i+1}^o \right)^T \mathbf{A}_{i+1}^o \Theta_i^c, \\ \boldsymbol{\alpha}_{i+1} &= -\alpha_i \tilde{\mathbf{A}}_{i+1}^o \left(\Theta_i^r \right)^T, \\ \boldsymbol{\beta}_{i+1} &= -\beta_i \mathbf{A}_{i+1}^o \Theta_i^c, \end{aligned}$$

together with Eq. (5.5). The nonvanishing entries in the change of basis matrices read

$$\begin{cases} \mathbf{A}_i^r = \boldsymbol{\alpha}_{i+1}^T \mathbf{A}_{i+1}^o \\ \mathbf{A}_{ii} = \alpha_i \end{cases} \quad \begin{cases} \tilde{\mathbf{A}}_i^r = \boldsymbol{\beta}_{i+1}^T \tilde{\mathbf{A}}_{i+1}^o \\ \tilde{\mathbf{A}}_{ii} = \beta_i. \end{cases}$$

It should be noted that the solution is still not unique because Eq. (5.5) imposes only a constraint on the product $\alpha_i \beta_i$. Once either α_i or β_i is fixed, all the unknown entries in the matrices \mathbf{A} and $\tilde{\mathbf{A}}$ can be uniquely determined. In other words, the normalization of the primal (resp. dual) functions is arbitrary, but once this is fixed, also the normalization of the dual (resp. primal) functions is determined. This flexibility allows, for example, to obtain biorthogonal border scaling functions and wavelets with the same L^2 -norm as for the internal functions. This can be a useful property when deriving adapted representations through thresholding of the wavelet coefficients, because it allows to use the same strategy for all coefficients.¹⁶

6. An Application

We illustrate in this section the excellent localization of the proposed construction. To this end, we compare the number of wavelet coefficients required to represent at a given accuracy a function characterized by regions of fast variations located either at the boundary or at internal points of the domain. More precisely, we will

Table 2. B-splines (3,5)

δ	N^b	$N^{1/2}$	$N^{1/3}$	$\ e^b\ $	$\ e^{1/2}\ $	$\ e^{1/3}\ $
1×10^{-3}	32	32	32	3.05×10^{-3}	9.18×10^{-4}	1.31×10^{-3}
5×10^{-4}	38	32	33	9.45×10^{-4}	9.18×10^{-4}	1.14×10^{-3}
2×10^{-4}	42	38	40	3.48×10^{-4}	3.49×10^{-4}	4.07×10^{-4}
1×10^{-4}	44	40	45	2.57×10^{-4}	2.22×10^{-4}	1.86×10^{-4}
1×10^{-5}	50	48	51	2.43×10^{-4}	1.06×10^{-4}	1.06×10^{-4}
1×10^{-6}	56	56	55	2.42×10^{-4}	1.05×10^{-4}	1.06×10^{-4}
1×10^{-7}	60	58	61	2.42×10^{-4}	1.05×10^{-4}	1.06×10^{-4}
0	1024	1024	1024	2.42×10^{-4}	1.05×10^{-4}	1.06×10^{-4}

consider the following functions

$$\begin{aligned} f^b(x) &= \tanh(500x(1-x)), \\ f^{1/2}(x) &= \tanh(500(x-1/2)), \\ f^{1/3}(x) &= \tanh(500(x-1/3)). \end{aligned}$$

The first one is a model for a boundary layer, with sharp variations at both edges of the domain, while the second and the third ones have fast variations located at a dyadic point ($x = 1/2$) and at an arbitrary point ($x = 1/3$), respectively.

We consider the full expansion (we omit the superscripts in the following)

$$P_J f(x) = \sum_k c_{j_0, k} \varphi_{j_0, k}(x) + \sum_{j=j_0}^{J-1} \sum_k w_{jk} \psi_{jk}(x)$$

with a minimum and maximum refinement levels set to $j_0 = 4$ and $J = 10$. The adapted expansion is

$$P_J^\delta f(x) = \sum_k c_{j_0, k} \varphi_{j_0, k}(x) + \sum_{(j, k) \in \Lambda_\delta} w_{jk} \psi_{jk}(x), \quad (6.1)$$

where the set of retained coefficients is defined through absolute thresholding of the wavelet coefficients,

$$\Lambda_\delta = \{(j, k) : |w_{jk}| > \delta\},$$

with a fixed threshold δ . The total number of coefficients in the adapted expansion (6.1) is $N = \dim V_{j_0} + \#\Lambda_\delta$, where $\#\mathcal{A}$ denotes the cardinality of the set \mathcal{A} . Finally, the L^2 norm of the approximation error $\|e\| = \|f - P_J^\delta f\|$ is also computed for each value of δ .

Tables 1 and 2 show the number of coefficients needed to represent each of these functions at a given accuracy with the biorthogonal B-splines (2,4) and (3,5) systems, respectively. It can be concluded that, for both systems, the number of coefficients in the adapted representation is approximately the same when the fast variations are located either at the boundaries or at internal points in the domain.

Therefore, the proposed construction for the border wavelets is shown not to spoil the good behavior of wavelet decompositions on the real line when dealing with edges.

Acknowledgments

The authors would like to thank Claudio Canuto and Karsten Urban for many clarifying and useful discussions. This research has been partially supported by CNR ST/74 *Progetto Strategico Modelli e Metodi per la Matematica e l'Ingegneria*, and by the *European Commission* within the TMR project *Wavelets and Multiscale Methods in Numerical Analysis and Simulation*, No. ERB FMRX CT98 0184.

References

1. L. Anderson, H. Hall, B. Jawerth and G. Peters, *Wavelets on the closed subsets of the real line*, in **Topics in the Theory and Applications of Wavelets**, eds. L.L. Schumaker and G. Webb (Academic Press, Boston, 1994), pp. 1–61.
2. C. Canuto and A. Tabacco, *Multilevel decompositions of functional spaces*, *J. Fourier Anal. and Appl.* **3** (1997) 715–742.
3. C. Canuto and A. Tabacco, **Ondine biortogonali: teoria e applicazioni**, *Quaderni U.M.I. Vol. 46* (Pitagora Ed., 1999).
4. C. Canuto, A. Tabacco and K. Urban, *The wavelet element method Part I: Construction and Analysis*, *Appl. Comp. Harm. Anal.* **6** (1999) 1–52.
5. C. Canuto, A. Tabacco and K. Urban, *Numerical Solution of Elliptic Problems by the Wavelet Element Method*, in **Proceedings of the 2nd ENUMATH Conference**, eds. H.G. Boch et al. (World Scientific, Singapore, 1998), pp. 17–37.
6. A. Cohen, **Wavelet methods in numerical analysis**, to appear.
7. A. Cohen, I. Daubechies and J. Feauveau, *Biorthogonal bases of compactly supported wavelet*, *Comm. Pure and Appl. Math.* **45** (1992) 485–560.
8. A. Cohen, I. Daubechies and P. Vial, *Wavelets on the interval and fast wavelet transform*, *Appl. Comp. Harm. Anal.* **1** (1993) 54–81.
9. A. Cohen, R. Masson, *Adaptive Wavelet Methods for Elliptic PDE's – Preconditioning and Adaptivity*, *SIAM J. Sci. Comp.*, to appear.
10. W. Dahmen, *Stability of multiscale transformations*, *J. Fourier Anal. and Appl.* **4** (1996) 341–362.
11. W. Dahmen, *Wavelet and multiscale methods for operator equations*, *Acta Numerica* **6** (1997) 55–228.
12. W. Dahmen, A. Kunoth and K. Urban, *Biorthogonal Spline-Wavelets on the Interval — Stability and Moment Conditions*, RWTH Aachen, Preprint IGPM No.129, 1996, to appear in *Appl. Comp. Harm. Anal.*.
13. W. Dahmen, A. Kunoth and K. Urban, *Wavelets in Numerical Analysis and their quantitative properties*, in **Surface Fitting and Multiresolution Methods**, eds. A. Le Mehaute, C. Rabut, and L.L. Schumaker (Vanderbilt Univ. Press, Nashville, TN, 1997), pp. 93–130.
14. W. Dahmen and R. Schneider, *Composite Wavelet Bases for Operator Equations*, RWTH Aachen, Preprint IGPM No. 133, 1996, to appear in *Math. Comp.*.
15. I. Daubechies, **Ten Lectures on Wavelets**, *CBMS-NSF Series in Applied Mathematics Vol. 61* (SIAM, Philadelphia, 1992).
16. R.A. DeVore, B. Jawerth and B.J. Lucier, *Image compression through wavelet transform*

- coding, *IEEE Trans. Information Th.* **38** (1992) 719–746.
17. S. Grivet-Talocia, **Wavelet-Based Numerical Schemes for the Solution of the Nonuniform Multiconductor Transmission Lines**, Ph.D. thesis, Dipartimento di Elettronica, Politecnico di Torino, 1998.
 18. S. Grivet-Talocia and F. Canavero, *Wavelet-Based Adaptive Solution for the Nonuniform Multiconductor Transmission Lines*, *IEEE Microwave and Guided Wave Letters* **8** (1998) 287–289.
 19. L. Levaggi and A. Tabacco, *Wavelets on the interval and related topics*, Dipartimento di Matematica, Politecnico di Torino, preprint 11 (1997).
 20. R. Masson, *Biorthogonal spline wavelets on the interval for the resolution of boundary problems*, *Math. Mod. Meths in Appl. Sci.* **6** (1996) 749–791.